Synchronization of coupled bistable chaotic systems: experimental study

By Alexander N. Pisarchik[1,*], Rider Jaimes-Reátegui[2] and
J. Hugo García-López[2]

[1]*Centro de Investigaciones en Optica, Loma del Bosque 115,
Lomas del Campestre, Leon 37150, Guanajuato, Mexico*
[2]*Universidad de Guadalajara, Centro Universitario de los Lagos,
Lagos de Moreno 47460, Jalisco, Mexico*

We carried out an experimental study of the synchronization of two unidirectionally coupled Rössler-like electronic circuits with two coexisting chaotic attractors. Different stages of synchronization are identified on the route from asynchronous motion to complete synchronization, as the coupling parameter is increased: intermittent asynchronous jumps between coexisting attractors; intermittent anticipating phase synchronization; and generalized synchronization in the form of subharmonic entrainment terminated by complete synchronization. All these regimes are analysed with time-series, power spectra and phase-space plots of the drive and response oscillators. The experimental study implicitly confirms the results of numerical simulations.

Keywords: synchronization; chaos; multistability; electronic circuits

1. Introduction

Synchronization of coupled chaotic systems has been intensively investigated (e.g. Pecora & Caroll 1990; Pikovsky *et al.* 2001; Boccaletti *et al.* 2002 and references therein). At first, the notion of synchronization was understood to be the coinciding of chaotic trajectories of coupled systems. Actually, this type of synchronization, which is observed in coupled identical systems, refers to *complete synchronization* (Murali & Lakshmanan 1994; Roy & Thornburg 1994; Sugawara *et al.* 1994). Later, it was realized that complete synchronization is only a particular type of synchronization. This type of synchronization has been widely used for secure communication with chaos (Hayes *et al.* 1993; Argyris *et al.* 2005). In general, synchronization implies a certain relation between functionals of two processes due to their interactions and can be observed not only in identical oscillators. To describe synchronization of non-identical systems, Rulkov *et al.* (1995) introduced a concept of *generalized synchronization*, which means the existence of some functional dependence between trajectories of coupled subsystems. This type of synchronization also includes the case of subharmonic entrainment of periodic or chaotic oscillations with the fundamental frequency of
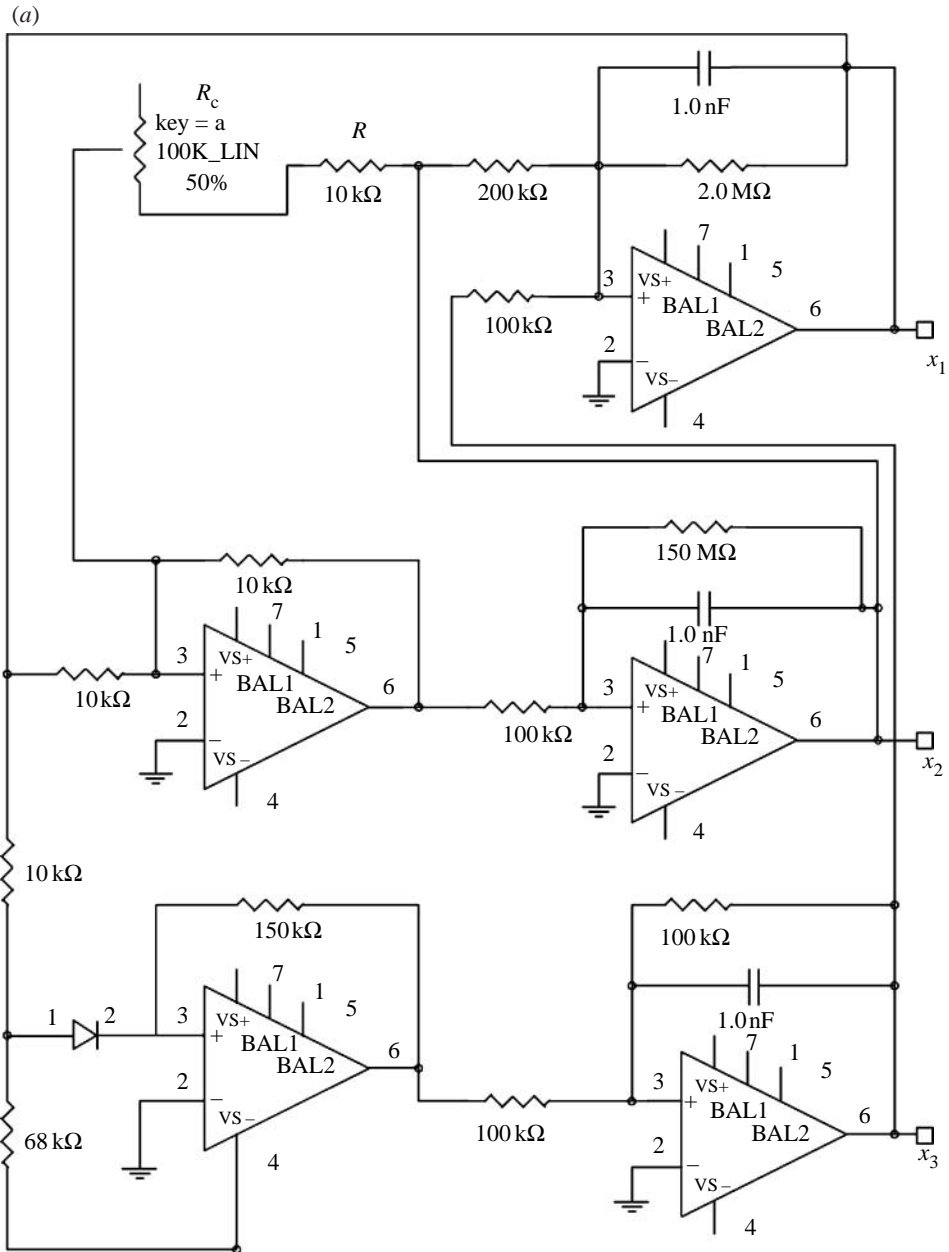
(a)

Figure 1. Electronic schemes of (a) drive, (b) response and (c) coupler circuits.

a driving system (Kocarev & Parlitz 1996). Rosenblum et al. (1996) identified another type of chaotic synchronization, *phase synchronization*, which implies a phase difference between chaotic oscillations that are locked within 2π. Later, other types of synchronization of coupled chaotic oscillators, such as *lag synchronization* and *anticipating synchronization*, were also identified by Rosenblum et al. (1997) and Voss (2000). All these types of synchronization have been detected in various experiments. Anticipating synchronization has
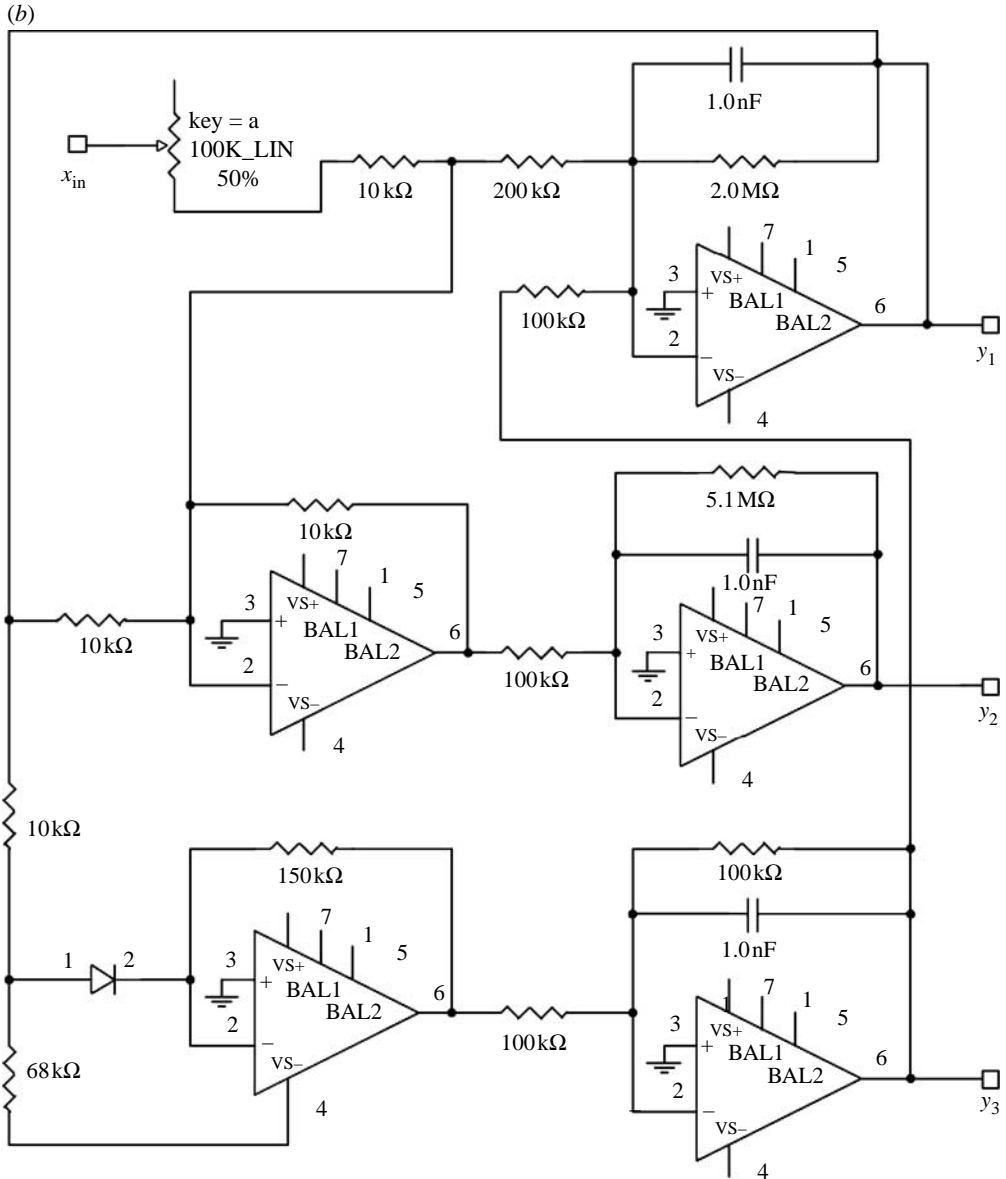
(b)

Figure 1. (*Continued.*)

recently been observed by Ciszak *et al.* (2003) in semiconductor lasers, but only in the presence of a time delay in coupling.

The majority of works on chaotic synchronization have been performed in monostable systems. However, it is known that many nonlinear systems have concurrent and coexisting attractors for the same parameter values. The dynamics of such multistable systems is defined by initial conditions. Recently, we have demonstrated numerically that the route from asynchronous motion to complete synchronization in two unidirectionally coupled bistable chaotic
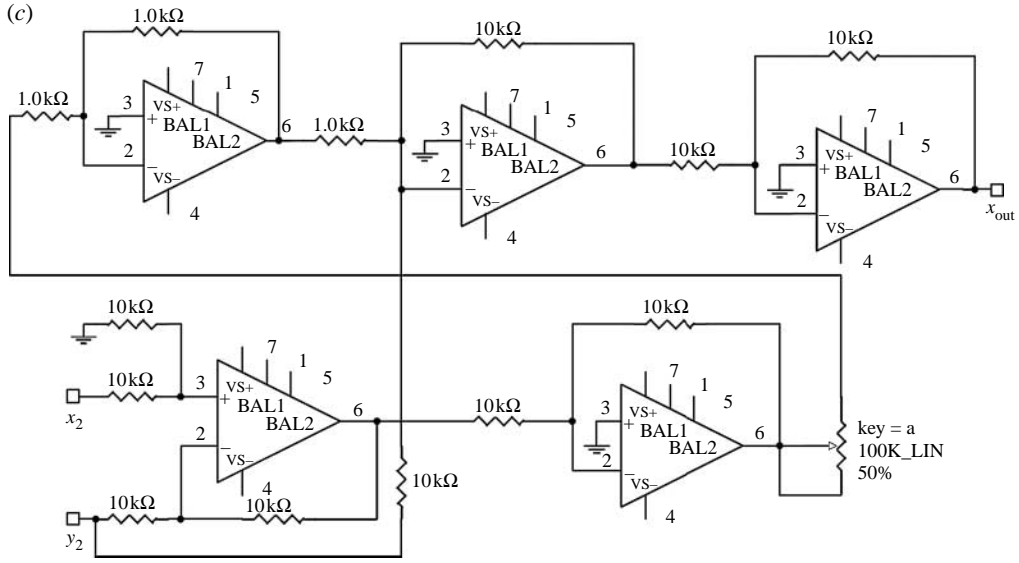
(*c*)

Figure 1. (*Continued.*)

systems is characterized by intermittent phase synchronization with anticipation (Pisarchik *et al.* 2006). This paper is devoted to the experimental study of synchronization in coupled bistable systems with coexisting chaotic attractors. As an example, we explore Rössler-like electronic circuits similar to those used previously by Carroll & Pecora (1995) in their first experiments on chaotic synchronization. We demonstrate different stages of chaotic synchronization depending on the coupling strength and discuss possible mechanisms underlying the synchronization phenomena.

2. Experimental set-up

We built the two identical electronic circuits shown in figure 1. One of them is the *drive circuit* (figure 1*a*) and another one is the *response circuit* (figure 1*b*). We also constructed the electronic circuit shown in figure 1*c* to provide unidirectional coupling between the drive and response oscillators. The parameters of all electronic components are indicated in figure 1*a*–*c*. These circuits are an analogue version of the following model equations:

$$\text{drive } \dot{\boldsymbol{x}} = \xi \begin{pmatrix} -\alpha x_1 & -\beta x_2 & -x_3 \\ x_1 & \gamma x_2 & 0 \\ g(x_1) & 0 & -x_3 \end{pmatrix}, \tag{2.1}$$

$$\text{response } \dot{\boldsymbol{y}} = \xi \begin{pmatrix} -\alpha y_1 & -\beta[y_2 + \varepsilon(x_2 - y_2)] & -y_3 \\ y_1 & \gamma[y_2 + \varepsilon(x_2 - y_2)] & 0 \\ g(y_1) & 0 & -y_3 \end{pmatrix} \text{ and} \tag{2.2}$$
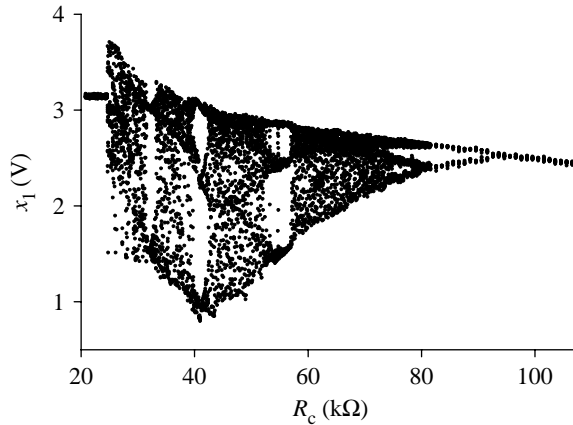
Figure 2. Experimental bifurcation diagram of peak voltage x_1 with resistance R_c as a control parameter.

$$g(x_1, y_1) = \left\{ \begin{array}{ll} 0, & \text{if } x_1, y_1 \leq 3 \\ \mu(x_1, y_1 - 3), & \text{if } x_1, y_1 > 3 \end{array} \right\}, \qquad (2.3)$$

where $\boldsymbol{x} = (x_1, \ x_2, \ x_3)$ and $\boldsymbol{y} = (y_1, \ y_2, \ y_3)$ are the state vectors; $\dot{\boldsymbol{x}} = \mathrm{d}\boldsymbol{x}/\mathrm{d}t$, $\dot{\boldsymbol{y}} = \mathrm{d}\boldsymbol{y}/\mathrm{d}t$, $\xi = 10^4 \, \mathrm{s}^{-1}$ is the time factor; $\alpha = 0.05$, $\beta = 0.5$, $\mu = 15$, $\varepsilon \in [0, \ 1]$ is the coupling strength; and γ is a variable parameter. The piecewise linear function equation (2.3) is determined by the diode D at the entrance of the operational amplifier in the x_3 loop. The amplifier is switched on when the voltage exceeds 3 V. The variable parameter $\gamma = R/R_c - 0.02$, where $R = 10 \, \mathrm{k}\Omega$ and R_c is a control resistance which can be varied between 27 and 200 kΩ.

3. Dynamics of one isolated circuit

When the drive and response circuits are not coupled ($\epsilon = 0$), each of them exhibits complex behaviour defined by control resistance R_c and the initial conditions. Let us, first, consider the dynamics of the single circuit shown in figure 1a. The experimental bifurcation diagram of output voltage x_1 versus control resistance R_c is shown in figure 2. We record this diagram several times by increasing and decreasing the control parameter. This procedure is equivalent to changing the initial conditions. For a large R_c, the behaviour of the single oscillator is similar to that of the system discovered by Rössler (1977), with a multiplicative first-order nonlinearity in the x_3 direction. The classical Rössler oscillator has a single saddle-node point located in the origin $(0, 0, 0)^{\mathrm{T}}$.

Similarly to the classical Rössler oscillator, our piecewise linear electronic circuit undergoes a cascade of period-doubling bifurcations followed by chaos when R_c is decreased (figure 2). Several periodic windows can also be distinguished in the diagram. At relatively large R_c ($R_c > 36 \, \mathrm{k}\Omega$), only Rössler-type chaos is observed. The chaotic attractor represents a so-called Rössler funnel (or an imperfect homoclinic orbit) around a saddle point. In our system, the lack of differentiability gives rise to coexistence of multiple attractors, cascades of period-adding bifurcations, period multiplication, homoclinic orbits,

jumps to chaos and destruction of all periodic orbits. These bifurcations, which are referred to as grazing bifurcations, are associated with portions of a trajectory being tangent to surfaces where the system is discontinuous. Such a complex behaviour appears only for small R_c when a second saddle point arises. The homoclinic orbits become perfect when a condition derived by Shil'nikov (1994) is fulfilled. Homoclinic dynamics of the system equation (2.1) has been analysed by Pisarchik & Jaimes-Reátegui (2005).

At relatively low values of the control parameter R_c, the bifurcation diagram represents a superposition of two different coexisting chaotic attractors, which merge in a crisis point at $R_c = 36$ kΩ. To study the synchronization of multistable systems, we fixed the control parameter at $R_c = 32$ kΩ, where our circuits exhibit the coexistence of two different chaotic attractors. Then, we chose the initial conditions (by switching on and off the power supply) for the drive and response circuits, so that their chaotic states would be different without coupling ($\varepsilon = 0$). The experimental time series for the three output voltages of the uncoupled circuits are shown in figure 3, and the corresponding phase trajectories are shown in figure 4. It is clear that the trajectories occupy different regions of the phase space. The natural frequencies of the two coexisting chaotic attractors are $f_1 = 0.82$ and $f_2 = 1.022$ kHz.

4. Synchronization stages

If two oscillators are identical and coupled by one variable, this variable can be considered as an external chaotic driver which increases the system dimension by one. In a unidirectionally coupled system with coexisting attractors, the response system has no effect on the dynamics of the drive system, and hence the drive system always remains in the same attractor.

For very weak coupling $\varepsilon < 0.5\%$, the driving signal has no influence on the response system and the states are defined only by the initial conditions. The two oscillators can be considered to be isolated and their trajectories occupy different regions of the phase space (see figures 3 and 4). However, a stronger coupling can change the global structure of the phase space of the response system owing to increasing dimension.

Let the initial states of the drive and response systems be chaotic attractors with natural frequencies $f_d = f_1$ and $f_r = f_2$. Synchronization can be characterized quantitatively as a difference between phases of corresponding variables of coupled systems (Boccaletti *et al.* 2002) that can be measured from experimental time series as $\Delta\phi = 2\pi(t_r^k - t_d^k)f_d$, where t_r^k and t_d^k are the times of the kth maxima of the coupled variables for the response and drive oscillators, respectively. While the coupling strength is increasing, the attractors in the response system can undergo different metamorphoses depending on the coupling strength.

(a) Asynchronous intermittent jumps

The response system becomes sensitive to the drive as soon as the coupling exceeds 0.5%, when random intermittent jumps between coexisting attractors occur. Examples of the experimental time series and the corresponding power spectra of the drive and response oscillations for different coupling strengths are shown in figure 5. When the response oscillator switches to the attractor similar to the drive system (figure 5a), driving frequency $f_1 = f_d$ appears in the power
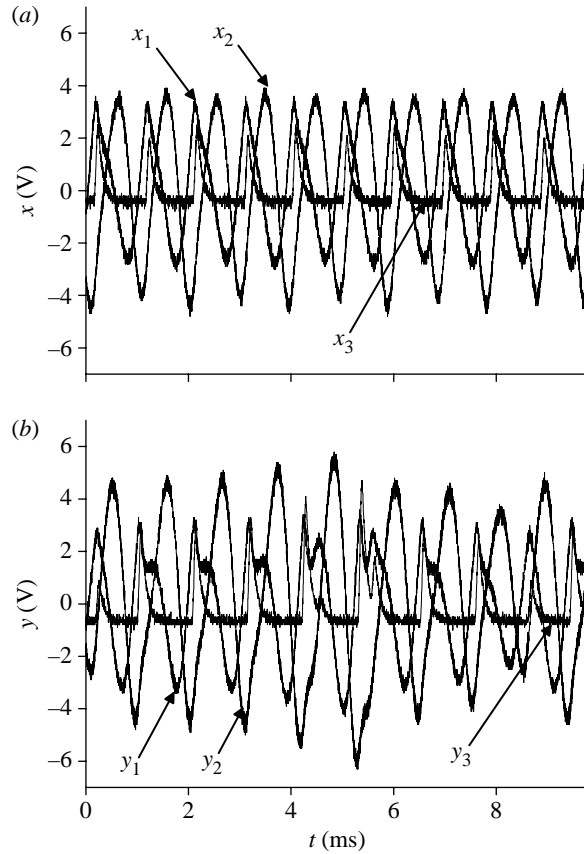
Figure 3. Experimental time-series of three variables for two different chaotic regimes in uncoupled circuits: (*a*) $x(\mathrm{V})$ and (*b*) $y(\mathrm{V})$. The time traces of different variables are shown by the arrows.
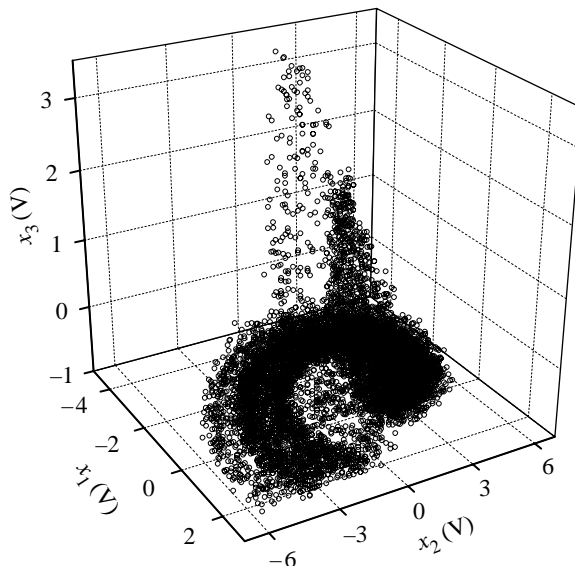

Figure 4. Phase-space trajectories of two different chaotic regimes shown by open and closed circles.
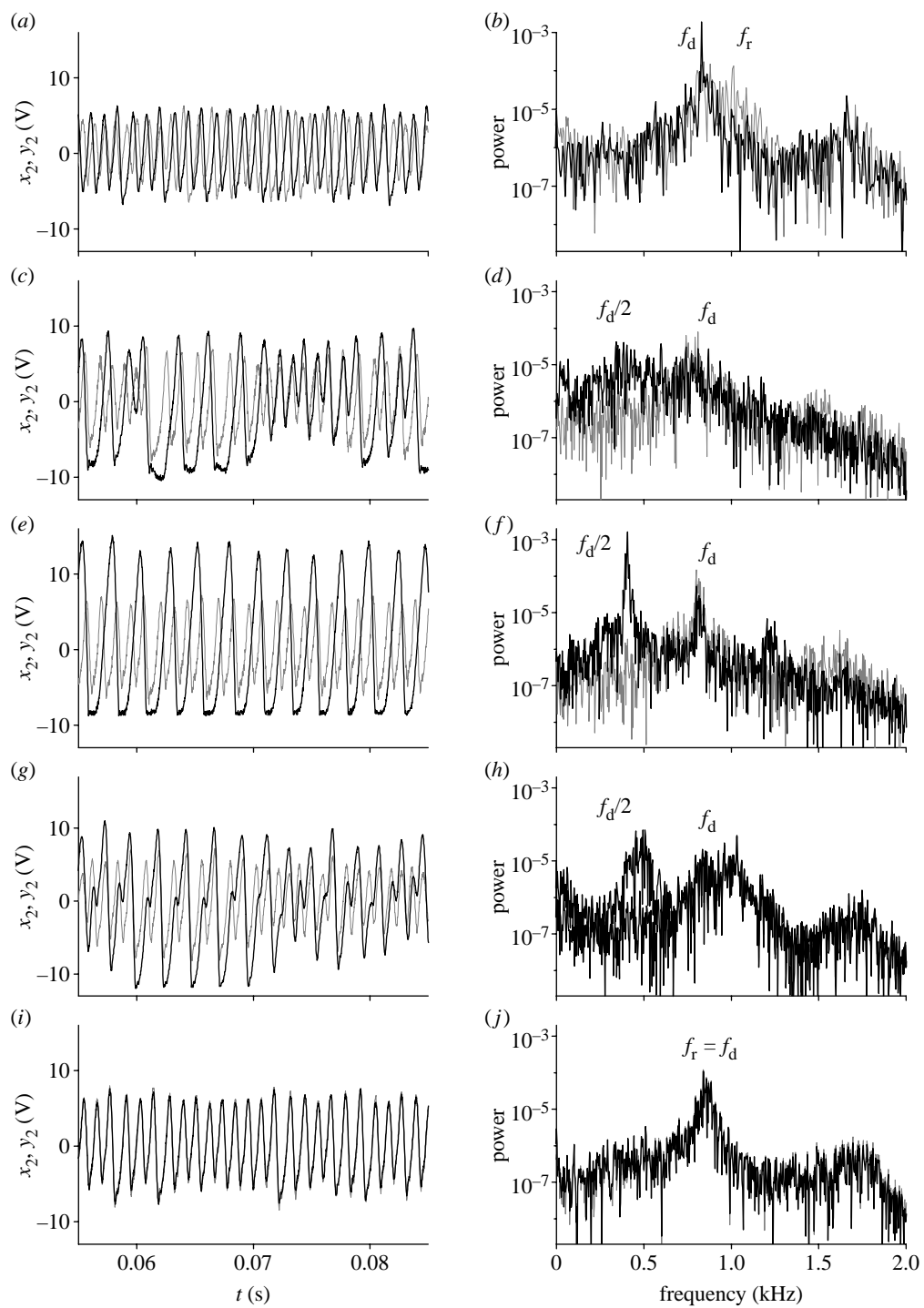
Figure 5. (*Caption opposite.*)

Figure 5. (*Opposite.*) Time-series (a,c,e,g,i) and the corresponding power spectra (b,d,f,h,j) demonstrating different synchronization stages for coupling parameters (a,b) $\varepsilon=0.006$, intermittent jumps between coexisting attractors, (c,d) $\varepsilon=0.24$, intermittent $1:2$ phase synchronization, (e,f) $\varepsilon=0.4$, $1:2$ phase synchronization, (g,h) $\varepsilon=0.7$, intermittent $1:2$–$1:1$ phase synchronization and (i,j) $\varepsilon=0.75$, $1:1$ or complete synchronization. The thin and thick lines correspond, respectively, to the drive and response oscillators.
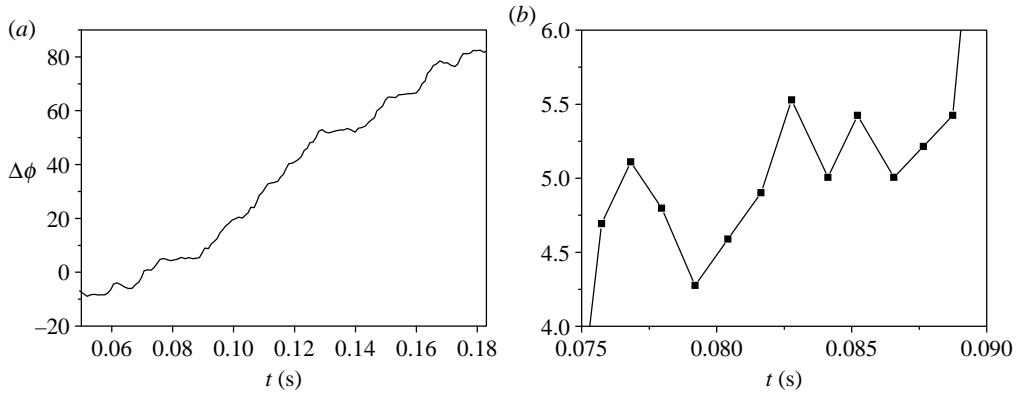

Figure 6. Phase difference between drive and response oscillations as a function of time for $\varepsilon=0.006$. (*a*) $\Delta\phi$ increases almost linearly with time when the two systems stay in different attractors. (*b*) Enlarged section demonstrating random fluctuations of $\Delta\phi$ on plateaus.

spectrum of the response system (middle part in figure 5*b*). Although at this stage no synchronization is detected, such an intermittent behaviour is a precursor of synchronization in multistable systems. The driving signal is too small to increase the system dimension and can be considered as external noise which just induces random switches between the coexisting attractors.

Figure 6*a* shows the phase difference $\Delta\phi$ as a function of time. Although this dependence has a tendency to increase linearly with time, one can distinguish short horizontal plateaus on which $\Delta\phi$ fluctuates in the 2π range (figure 6*b*). On the plateaus, the drive and response systems oscillate in antiphase, as seen in the middle part of figure 5*a*.

(*b*) *Intermittent phase synchronization*

A further increase in coupling parameter results in phase synchronization, which occurs only within the windows where the response system stays in the attractor similar to the attractor of the drive system. This synchronization regime appears when $\varepsilon>0.01$. The examples of the time series and phase difference $\Delta\phi(t)$ are shown in figure 7*a*,*b*. The fluctuation of $\Delta\phi$ on the plateaus is no longer random because its distribution is not Gaussian, rather it is Lorenzian. The duration of the synchronization windows is larger (figure 7*b*). Now, the response system is sensitive not only to some individual peaks of the drive oscillations, which induce switches between the coexisting attractors, but also to the phase of oscillations while the systems stay in the similar attractors.

It is remarkable that intermittent phase synchronization is always accompanied by anticipating synchronization, i.e. $\Delta\phi<0$ inside the synchronous
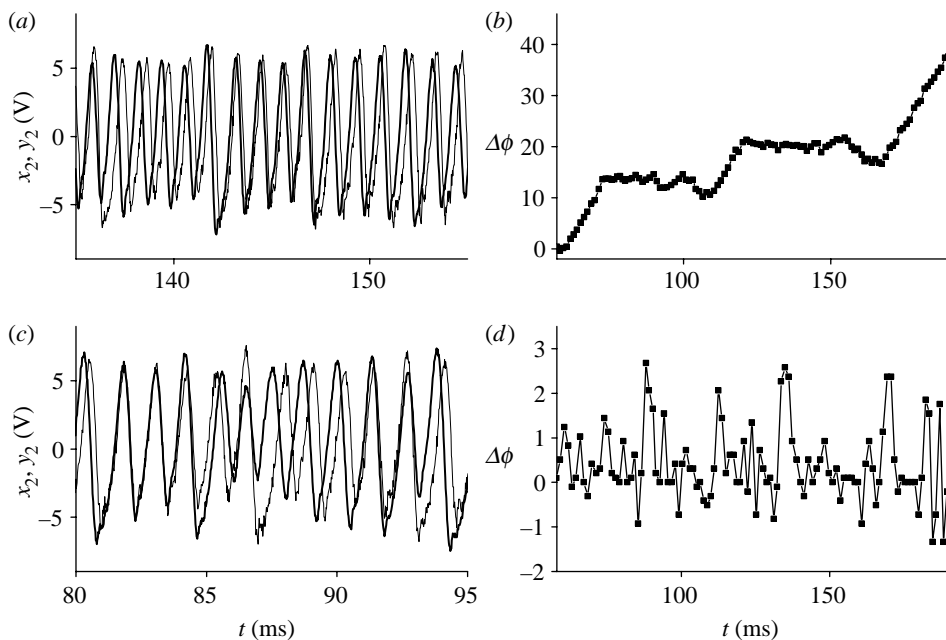
Figure 7. Time-series (a,c) and phase difference (b,d) for coupling parameters (a,b) $\varepsilon = 0.03$, intermittent anticipating phase synchronization and (c,d) $\varepsilon = 0.12$, combined attractor. The thin and thick lines indicate the time traces corresponding to the drive and response oscillators, respectively.

windows. Anticipating phase synchronization is clearly seen from the time-series in figure 7a, in which the time trace of the response system anticipates the driving trace. The averaged anticipation time is decreasing with increasing ε and eventually it approaches 0, as soon as phase synchronization becomes perfect, i.e. when $\Delta\phi \to 0$.

(c) Combined attractor

For stronger coupling parameters $(\varepsilon > 0.1)$, the dimension of the response system is no longer the same as the dimension of the drive system; instead, it is higher. Owing to the increasing dimension, the global structure of the phase space of the response system is completely different, and hence synchronization is hardly possible. The time-series and the phase dependence at this stage are shown in figure 7c,d; $\Delta\phi$ drifts in the vicinity of 0 (figure 7d). Sometimes, very large phase slips can occur, when $\Delta\phi$ rises up to a half of the averaged period of the drive oscillations (as seen in figure 7c) although windows of perfect phase synchronization ($\Delta\phi = 0$) can appear as well. The dynamical behaviour is very similar to that of coupled non-identical (even structurally different) systems.

(d) Generalized synchronization

While the coupling strength is further increasing, the attractors in the response system can undergo a homeomorphism. This phenomenon was discovered first by Afraimovich *et al.* (1986) and was later generalized by

Rulkov *et al.* (1995) to a system of coupled non-identical oscillators. In the case of multistability, identical systems in different attractors can be considered as different systems. However, generalized synchronization is possible. Mathematically, this may be formulated as follows. *Generalized synchronization* in coupled multistable systems occurs for the attractor $A_i \subset \mathbb{R}^m$ of the drive system and a new homeomorphic attractor $B_j \subset \mathbb{R}^n$ of the response system ($i = 1, ..., p$ and $j = 1, ..., q$ being the attractor numbers and m and n being the dimensions of the drive and response systems, respectively), if an attracting synchronization set $M = \{(\boldsymbol{x}, \boldsymbol{y}) \in B_j \times \mathbb{R}^n : \boldsymbol{y} = \boldsymbol{H}(\boldsymbol{x})\}$ exists that is given by some function $\boldsymbol{H} : B_j \rightarrow A_i \subset \mathbb{R}^n$ and that possesses an open basin $D \supset M$ such that $\lim_{t \rightarrow \infty} \|\boldsymbol{y}(t) - \boldsymbol{H}(\boldsymbol{x}(t))\| = 0 \quad \forall (\boldsymbol{x}(0), \boldsymbol{y}(0)) \in D$. This definition also includes the case of subharmonic entrainment of periodic or chaotic oscillations with fundamental frequency $f(A_i)$. For example, the entrainment with ratio $f(B_j) : f(A_i) = 1 : q$ ($q > 1$) results from q attractors in the response system.

The increasing coupling parameter above 20% gives rise to a period-doubling bifurcation for the chaotic attractor similar to the driving attractor that can lead to intermittent jumps to this new attractor. As a result, slips of period-doubling oscillations arise in the time-series (figure 5*c*), and frequency $f_\mathrm{d}/2$ appears in the power spectrum (figure 5*d*). The period-doubling oscillations are phase synchronized with the drive in the $1 : 2$ ratio. We refer to this type of synchronization as *intermittent period-doubling phase synchronization*. As ε is increased, the period-doubling windows are enlarging and, eventually, the system becomes perfectly phase synchronized in the period-doubling regime, i.e. *period-doubling phase synchronization* takes place as shown in figure 5*e*. Such a frequency entrainment is the manifestation of generalized synchronization. Recently, Pisarchik & Barmenkov (2005) observed a similar locking effect of the natural frequency to the period-doubling frequency of driving oscillations in a fibre laser with pump modulation.

(*e*) *Complete synchronization*

Although the coupling is increasing above 60%, the period-doubling regime is transforming into a period-one regime, while phase synchronization is being conserved. The transition from $1 : 2$ frequency locking to $1 : 1$ frequency locking is shown in figure 5*g,h* with the time-series and power spectra. The chaotic attractor of the response system is converted into a chaotic attractor similar to the drive system. The peaks of the natural frequencies in the power spectrum are broadened. This indicates a final stage on the route to complete synchronization that eventually occurs for $\varepsilon > 0.75$ owing to the decreasing dimensions of the response system. Any trajectory of the response system converges to the same trajectory as the drive system, i.e. $\boldsymbol{y}(t) - \boldsymbol{x}(t) = 0$ for $t \rightarrow \infty$, which results in the reducing number of coexisting attractors up to a single attractor, identical to the attractor of the drive system. This case is shown in figure 5*i,j*.

It is worth mentioning that synchronization of coupled systems is closely related to the problem of nonlinear control, although the goals may sometimes be different (Kapitaniak 1994). In unidirectionally coupled systems, the drive system acts as a controller for the response system to attract its trajectory to a

desired trajectory defined by the controller. The synchronization problem for coupled multistable systems can be considered as a problem of controlling multistability or inter-attractor control.

5. Discussion

The synchronization phenomena described above can be interpreted in terms of periodic orbit structures of the driver and responder subsystems (Barreto *et al.* 2000). Many papers describe synchronization of coupled chaotic systems in the framework of an invariant synchronization manifold $\Im$, which can easily be found in coupled systems with symmetry, such as in our case. The results described above confirm the existence of $\Im$ within a plane of symmetry for a wide range of coupling. The variables of the drive and response systems evolve identically on $\Im$ and hence the systems display identical synchrony. However, owing to multistability in the coupled subsystems, $\Im$ can become extremely complicated and be destroyed as the coupling parameter is decreased.

In figure 8 we show the evolution of the attractor as the coupling parameter ε is decreased. Since the coupled oscillators are identical, the synchronization manifold $\Im$ is simply the line $x = y$. It is invariant and attracting at $\varepsilon = 1$ and remains so for $\varepsilon > 0.75$ (figure 8a) until a *bubbling bifurcation* occurs at critical value $\varepsilon_{b1} \approx 0.74$. For $\varepsilon < \varepsilon_{b1}$, $\Im$ is no longer invariant. Upon decreasing ε, the trajectory first makes finite size intermittent short-lived excursions away from $\Im$ (figure 8b), i.e. a *bubbling transition* occurs. Before the bubbling transition takes place, the chaotic attractor is asymptotically stable. At the bubbling bifurcation, the orbit within $\Im$ loses transverse stability and after the bifurcation the attractor is only an attractor in the weaker sense of being a Milnor (measure) attractor. Such an *emergence* of the intermittent bursts of chaotic trajectories away from the previously constrained attractor is the generic qualitative manifestation of the bubbling transition in a physical system with an invariant manifold, and this is often caused by the presence of symmetries in the system. A similar behaviour has been observed previously in monostable coupled chaotic systems (Ashwin *et al.* 1994; Venkataramani *et al.* 1996). In our case of the system with two coexisting chaotic attractors, the bubbling bifurcation at which the orbit in $\Im$ loses transverse stability is accompanied by a *period-doubling (pitchfork) bifurcation* at which a new chaotic attractor $\aleph$ is created outside of $\Im$. The trajectory spends a long time in the vicinity of $\Im$, but makes occasional excursions to another coexisting attractor. This leads to the attractor smearing (fattening) that can be seen in figure 8b. As ε is further decreased, the chaotic attractor $\Im$ itself becomes transverse unstable via a *blowout bifurcation* (Ott & Sommerer 1994), while the period-doubling attractor $\aleph$ becomes stable. One can see in figure 8c that this new 1:2 synchronization manifold has a more complicated structure; the oscillations display generalized synchrony with a 1:2 frequency ratio.

As the coupling is further reduced, the next desynchronization cycle is initiated via the next bubbling transition, which appears at critical value $\varepsilon_{b2} \approx 0.32$. The period-doubling orbit loses its transverse stability, making excursions away from $\aleph$ (figure 8d). Finally, the attractor $\aleph$ itself becomes transverse unstable in the next blowout bifurcation that leads to the attractor
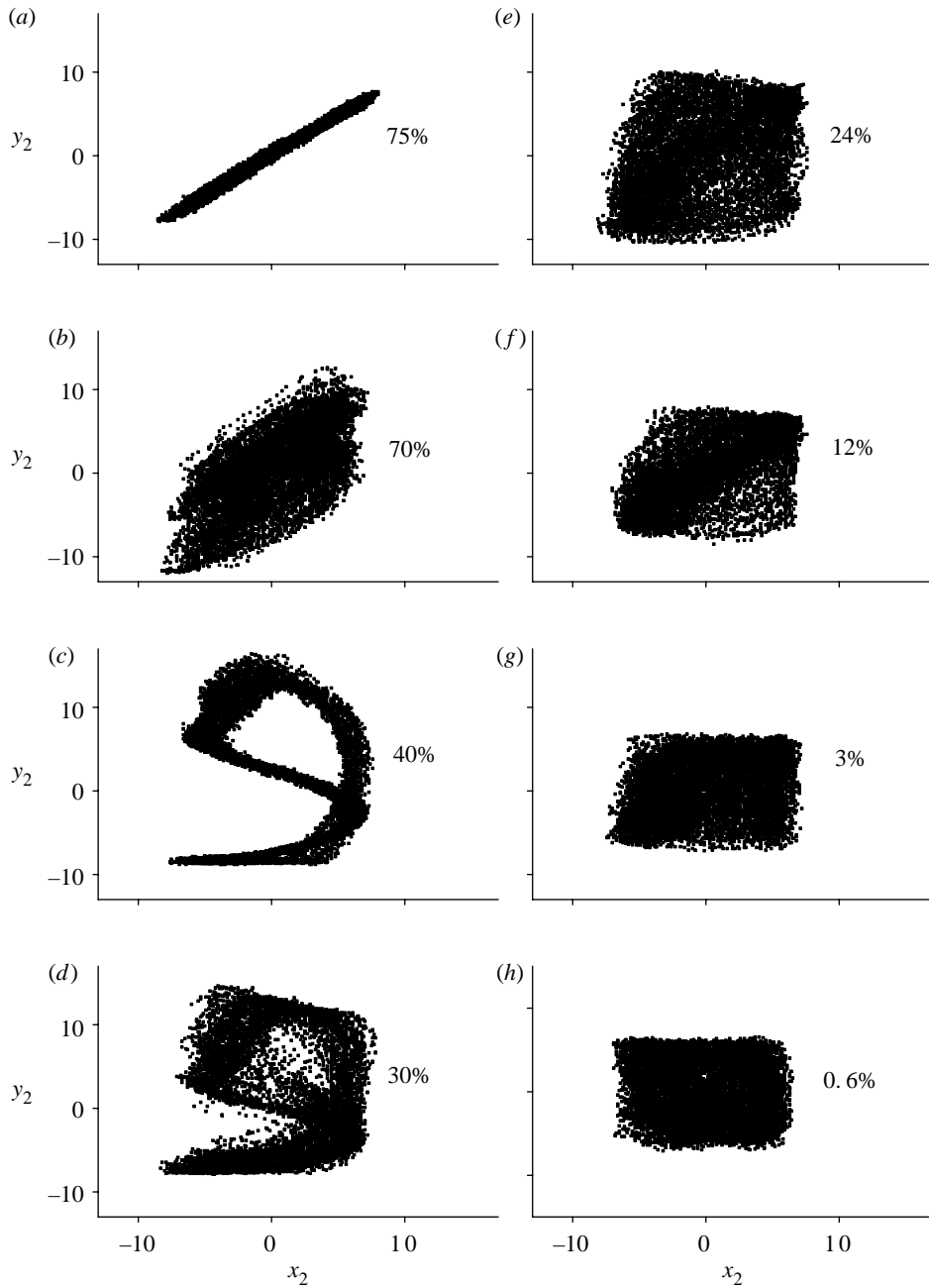
Figure 8. Attractor evolution in phase space as coupling is decreased for diffusively coupled circuits. The coupling parameter ε (in %) is indicated near each plot: (*a*) 75%, (*b*) 70%, (*c*) 40%, (*d*) 30%, (*e*) 24%, (*f*) 12%, (*g*) 3% and (*h*) 0.6%.

smearing, as seen in figure 8*e*. For smaller ε (figure 8*f*,*g*), the state variables may still be functionally related, resulting in generalized synchronization. However, due to the coexistence of attractors with different, not multiple, frequencies, this

function can be extremely complicated, and the identification of bubbling and blowout bifurcations is problematic. At very low couplings, no synchronization is observed (figure 8*h*).

6. Conclusions

In this work we have studied experimentally the route from asynchronous behaviour to complete synchronization in unidirectionally coupled oscillators with coexisting chaotic attractors. We have built two electronic Rössler-like circuits and shown that the coexistence of attractors results from nonlinearity due to a piecewise linear dependence in one of the system variables. We have demonstrated experimentally different synchronization stages on the route from asynchronous motion to complete synchronization. This scenario includes intermittent anticipating phase synchronization and period-doubling phase synchronization. The latter is a particular case of generalized synchronization. We have demonstrated the bubbling transitions as the emergence of intermittent bursts of chaotic trajectories away from the previously constrained attractor to a newly created attractor intermittently synchronized with the drive. Such a behaviour of multistable coupled systems contains combined features inherent to both identical and non-identical coupled systems. Furthermore, the coupled multistable systems also have specific features that are not observed in monostable coupled systems, for example two-state on–off intermittent phase synchronization, a shift of the fundamental frequency of one of the chaotic attractors and period-doubling phase synchronization.

Similar bifurcation scenarios on the route to complete synchronization, as the coupling parameter was increased, have also been found in the cases of coexistence of one periodic and one chaotic attractors and two periodic attractors with different fundamental frequencies. Although the dynamics in these cases were not so rich as in the case of two coexisting chaotic attractors, the synchronization features mentioned above are common. We believe that the results described in this paper are quite general for a wide class of coupled bistable and multistable systems. The experimental results implicitly confirm the results of numerical simulations (Pisarchik *et al.* in press). Synchronization of bistable chaotic systems may be of interest for communication applications if the information is encrypted into proper switches between coexisting attractors or into a qualitative change of a synchronization regime.

References

Afraimovich, V. S., Verichev, N. N. & Rabinovich, M. I. 1986 Stochastic synchronization of oscillation in dissipative systems. *Radiophys. Quantum Electron.* **29**, 795–803. (doi:10.1007/BF01034476)

Argyris, A. *et al.* 2005 Chaos-based communications at high bit rates using commercial fibre-optic links. *Nature* **438**, 343–346. (doi:10.1038/nature04275)

Ashwin, P., Buescu, J. & Stewart, I. 1994 Bubbling of attractors and synchronization of chaotic oscillators. *Phys. Lett. A* **193**, 126–139. (doi:10.1016/0375-9601(94)90947-4)

Barreto, E., So, P., Gluckman, B. J. & Schiff, S. J. 2000 From generalized synchrony to topological decoherence: emergent sets in coupled chaotic systems. *Phys. Rev. Lett.* **84**, 1689–1692. (doi:10.1103/PhysRevLett.84.1689)

Boccaletti, S., Kurths, J., Osipov, G., Valladares, D. L. & Zhou, C. 2002 The synchronization of chaotic systems. *Phys. Rep.* **366**, 1–101. (doi:10.1016/S0370-1573(02)00137-0)

Carroll, T. & Pecora, L. 1995 *Nonlinear dynamics in circuits.* Singapore: World Scientific Publishing.

Ciszak, M., Calvo, O., Masoller, C., Mirasso, C. R. & Toral, R. 2003 Anticipating the response of excitable systems driven by random forcing. *Phys. Rev. Lett.* **90**, 204102. (doi:10.1103/PhysRevLett.90.204102)

Hayes, S., Grebogi, C., Ott, E. & Mark, A. 1993 Communicating with chaos. *Phys. Rev. Lett.* **70**, 3031–3034. (doi:10.1103/PhysRevLett.70.3031)

Kapitaniak, T. 1994 Synchronization of chaos using continuous control. *Phys. Rev. E* **50**, 1642–1644. (doi:10.1103/PhysRevE.50.1642)

Kocarev, L. & Parlitz, U. 1996 Generalized synchronization, predictability, and equivalence of unidirectionally coupled dynamical systems. *Phys. Rev. Lett.* **76**, 1816–1819. (doi:10.1103/PhysRevLett.76.1816)

Murali, K. & Lakshmanan, M. 1994 Drive-response scenario of chaos synchronization in identical nonlinear systems. *Phys. Rev. E* **49**, 4882–4885. (doi:10.1103/PhysRevE.49.4882)

Ott, E. & Sommerer, J. A. 1994 Blowout bifurcations: the occurrence of riddled basins and on–off intermittency. *Phys. Lett. A* **188**, 39–47. (doi:10.1016/0375-9601(94)90114-7)

Pecora, L. M. & Carroll, T. L. 1990 Synchronization in chaotic systems. *Phys. Rev. Lett.* **64**, 821–824. (doi:10.1103/PhysRevLett.64.821)

Pikovsky, A., Rosenblum, M. & Kurths, J. 2001 *Synchronization: a universal concept in nonlinear science.* New York, NY: Cambridge University Press.

Pisarchik, A. N. & Barmenkov, Y. O. 2005 Locking of self-oscillation frequency by pump modulation in an erbium-doped fiber laser. *Opt. Commun.* **254**, 128–137. (doi:10.1016/j.optcom.2005.05.028)

Pisarchik, A. N. & Jaimes-Reátegui, R. 2005 Homoclinic orbits in a piecewise linear Rössler circuit. *J. Phys.: Conf. Ser.* **23**, 122–127. (doi:10.1088/1742-6596/23/1/014)

Pisarchik, A. N., Jaimes-Reátegui, R., Villalobos-Salazar, J. R., García-López, J. H. & Boccaletti, S. 2006 Synchronization of chaotic systems with coexisting attractors. *Phys. Rev. Lett.* **96**, 244102. (doi:10.1103/PhysRevLett.96.244102)

Pisarchik, A. N., Jaimes-Reátegui, R., Villalobos-Salazar, J. R. & García-López, J. H. In press. Synchronization of multistable systems. *Int. J. Bifurcat. Chaos.*

Rosenblum, M. G., Pikovsky, A. S. & Kurths, J. 1996 Phase synchronization of chaotic oscillators. *Phys. Rev. Lett.* **76**, 1804–1807. (doi:10.1103/PhysRevLett.76.1804)

Rosenblum, M. G., Pikovsky, A. S. & Kurths, J. 1997 From phase to lag synchronization in coupled chaotic oscillators. *Phys. Rev. Lett.* **78**, 4193–4196. (doi:10.1103/PhysRevLett.78.4193)

Rössler, O. E. 1977 Chaos in abstract kinetics: two prototypes. *B. Math. Biol.* **39**, 275–289.

Roy, R. & Thornburg Jr, K. S. 1994 Experimental synchronization of chaotic lasers. *Phys. Rev. Lett.* **73**, 2009–2012. (doi:10.1103/PhysRevLett.72.2009)

Rulkov, N. F., Sushchik, M. M., Tsimring, L. S. & Abarbanel, H. D. I. 1995 Generalized synchronization of chaos in directionally coupled chaotic systems. *Phys. Rev. E* **51**, 980–983. (doi:10.1103/PhysRevE.51.980)

Shil'nikov, L. P. 1994 Chua's circuit: rigorous and future problems. *Int. J. Bifurcat. Chaos* **4**, 489–520. (doi:10.1142/S021812749400037X)

Sugawara, T., Tachikawa, M., Tsukamoto, T. & Shimizu, T. 1994 Observation of synchronization in laser chaos. *Phys. Rev. Lett.* **72**, 3502–3505. (doi:10.1103/PhysRevLett.72.3502)

Venkataramani, S. C., Hunt, B. R., Ott, E., Gauthier, D. J. & Bienfang, J. C. 1996 Transitions to bubbling of chaotic systems. *Phys. Rev. Lett.* **77**, 5361–5364. (doi:10.1103/PhysRevLett.77.5361)

Voss, H. U. 2000 Anticipating chaotic synchronization. *Phys. Rev. E* **61**, 5115–5119. (doi:10.1103/PhysRevE.61.5115)